A Component-Wise Approach for the Failure Analysis of Composite Structures

E. Carrera*, M. Maiarù† and M. Petrolo‡

Mechanical and Aerospace Engineering Department, Politecnico di Torino, Torino, Italy

This paper proposes a novel approach for the FE analysis of composites which is able to provide accurate stress fields with very low computational costs. 1D refined theories were employed and attention was given to fiber-reinforced composite structures. The structural models were derived in the framework of the Carrera Unified Formulation (CUF) which provides hierarchical higher-order structural models with arbitrary expansion orders. The proposed novel approach is referred to as *Component-Wise* (CW). Within the CW approach, different scale components (fiber, matrix, laminae and laminates) can be simultaneously modeled in a structural model with separate sets of unknown displacement variables and material characteristics. These characteristics are homogenized at the interface level. In this work, CW was used for failure analyses by implementing well-known failure criteria. The results obtained in this paper show the enhanced capabilities of the present CW formulation for the failure analysis of composite structures since very accurate displacement/stress fields were obtained with low computational costs.

I. Introduction

Composites provide significant advantages in performance, efficiency and costs; thanks to these features, the application of composite structures is increasing in many engineering fields, such as aerospace, naval and mechanical engineering. Although the adoption of composites is increasing, there are still open issues to be investigated in order to improve the available design technologies. Damage and failure mechanisms in composites are of particular interest and complexity since these mechanisms are heavily affected by many parameters such as geometry, lay-up and boundary conditions.[1] Furthermore, composite structures are characterized by different length scales. In the case of fiber reinforced composites, the scales involved may be the sub-lamina (fiber and matrix), the lamina and the laminate. The proper modeling of these scales and their interactions is of primary importance to detect reliable stress fields and to evaluate the structural integrity of a composite structure. Different methodologies are available to compute accurate stress/strain fields in a laminated structure, some of these techniques are discussed hereafter.

The adoption of 3D solid finite elements enhances the analysis of 1D and 2D composite components. 3D elements can be employed to model fiber and matrix or the layer of a laminated structure. The main drawback of this approach is related to the enormous computational costs that 3D solid models could require in real applications with a high number of layers.

Refined 2D (plate/shell) and 1D (beam) models represent another tool for the structural analysis of laminates. Different refining approaches have been proposed, such as higher-order models,[2] Zig-zag theories[3,4] and Layer-Wise (LW) approaches.[5,6]

Global-local methodologies can be also employed in composite structure analyses. Typical examples are the superimposition of Equivalent Single Layer models (ESL) and LW[7] or the use of the Arlequin method to combine higher- and lower-order theories.[8,9]

*Professor, Mechanical and Aerospace Engineering Department, Politecnico di Torino, Corso Duca degli Abruzzi, 24, 10129 Torino, Italy, erasmo.carrera@polito.it

†PhD Student, Mechanical and Aerospace Engineering Department, Politecnico di Torino, Corso Duca degli Abruzzi, 24, 10129 Torino, Italy, marianna.maiaru@polito.it

‡Research Assistant, Mechanical and Aerospace Engineering Department, Politecnico di Torino, Corso Duca degli Abruzzi, 24, 10129 Torino, Italy, marco.petrolo@polito.it

Multiscale methods are finding increasing application and development. An overview on the available multiscale techniques has been provided by Lu and Kaxiras.[10] A possible approach is based on the use of the molecular dynamics at the nano-scale level, the Representative Volume Elements at micro-level and structural elements at the macro-scale. The Generalized Method of Cell (GMC)[11,12] is an important tool in the multiscale framework.
A novel technique is presented in this paper which is based on a unified formulation for 1D structural elements referred to as the Carrera Unified Formulation[13–15] (CUF). 1D CUF models have enhanced capabilities for the detection of 3D-like results with very low computational costs. The approach proposed in this paper is referred to as *Component-wise* (CW).[16] Component-wise means that each typical component of a laminate (i.e. laminae, fibers and matrices) can be separately modeled with its own set of unknown variables and material characteristics by means of a unique formulation. Moreover, in a given model different scale components can be used simultaneously, that is, homogenized laminates and laminae can be interfaced with fibers and matrices. In the CW approach, model capabilities can be tuned by 1. choosing in which part of the structure a more detailed model has to be used; 2. setting the order of the structural model to be used. A graphic description of the present model capabilities is provided in Figure 1. Such a model can be seen

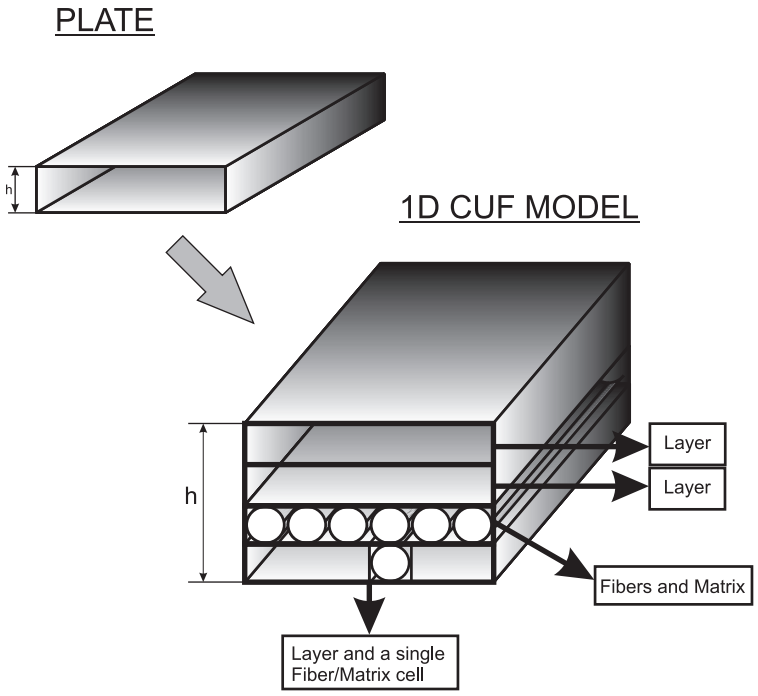

Figure 1. An example of component-wise approach

as a 'global-local' model since it can be used either to create a *global* model by considering the full laminate or to obtain a *local* model to look for accurate strain/stress distributions in those parts of the structure which could most likely be affected by failure. In other words, the present modeling approach deals with progressively refined models up to the fiber and matrix scales.
This work presents a description of CUF and CW and their application to the failure analysis of composites by the implementation of well-known failure criteria.

II. CUF 1D Formulation

The transposed displacement vector is defined as

$$\mathbf{u}(x,y,z) = \left\{ \begin{array}{ccc} u_x & u_y & u_z \end{array} \right\}^T \tag{1}$$

where x, y, and z are orthonormal axes as shown in Fig. 2. The cross-section of the structure is Ω, the

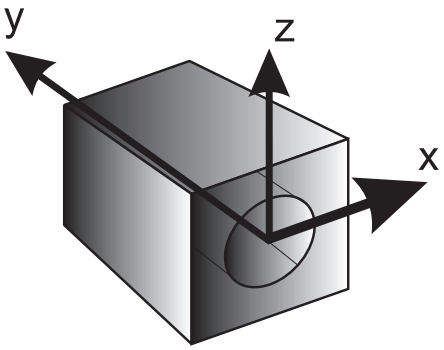

Figure 2. Coordinate frame

longitudinal axis is $0 \leq y \leq L$. Stress, $\boldsymbol{\sigma}$, and strain, $\boldsymbol{\epsilon}$, components are grouped as

$$\begin{aligned} \boldsymbol{\sigma}_p &= \left\{ \begin{array}{ccc} \sigma_{zz} & \sigma_{xx} & \sigma_{zx} \end{array} \right\}^T, \quad \boldsymbol{\epsilon}_p = \left\{ \begin{array}{ccc} \epsilon_{zz} & \epsilon_{xx} & \epsilon_{zx} \end{array} \right\}^T \\ \boldsymbol{\sigma}_n &= \left\{ \begin{array}{ccc} \sigma_{zy} & \sigma_{xy} & \sigma_{yy} \end{array} \right\}^T, \quad \boldsymbol{\epsilon}_n = \left\{ \begin{array}{ccc} \epsilon_{zy} & \epsilon_{xy} & \epsilon_{yy} \end{array} \right\}^T \end{aligned} \tag{2}$$

The subscript "n" stands for terms lying on the cross-section, while "p" stands for terms lying on planes which are orthogonal to Ω.
Strains are obtained as

$$\begin{aligned} \boldsymbol{\epsilon}_p &= \boldsymbol{D}_p \mathbf{u} \\ \boldsymbol{\epsilon}_n &= \boldsymbol{D}_n \mathbf{u} = (\boldsymbol{D}_{np} + \boldsymbol{D}_{ny}) \mathbf{u} \end{aligned} \tag{3}$$

where $\boldsymbol{D}_p$ and $\boldsymbol{D}_n$ are differential operators whose explicit expression is not reported here for the sake of brevity, it can be found in Carrera et al.[17] Constitutive laws are introduced to obtain stress components,

$$\boldsymbol{\sigma} = \tilde{\boldsymbol{C}} \boldsymbol{\epsilon} \tag{4}$$

According to Eq.s 2, the previous equation becomes

$$\begin{aligned} \boldsymbol{\sigma}_p &= \tilde{\boldsymbol{C}}_{pp} \boldsymbol{\epsilon}_p + \tilde{\boldsymbol{C}}_{pn} \boldsymbol{\epsilon}_n \\ \boldsymbol{\sigma}_n &= \tilde{\boldsymbol{C}}_{np} \boldsymbol{\epsilon}_p + \tilde{\boldsymbol{C}}_{nn} \boldsymbol{\epsilon}_n \end{aligned} \tag{5}$$

where $\tilde{\boldsymbol{C}}_{pp}$, $\tilde{\boldsymbol{C}}_{pn}$, $\tilde{\boldsymbol{C}}_{np}$, and $\tilde{\boldsymbol{C}}_{nn}$ are the material coefficient matrices whose explicit expressions is not reported here for the sake of brevity, it can be found in Carrera et al.[17]

A. Hierarchical Variable Kinematics: TE and LE models

In the CUF framework, the displacement field is the expansion of generic functions F_τ,

$$\mathbf{u} = F_\tau \mathbf{u}_\tau, \qquad \tau = 1, 2, ..., M \tag{6}$$

where F_τ vary above the cross-section. $\mathbf{u}_\tau$ is the displacement vector and M stands for the number of terms of the expansion. According to the Einstein notation, the repeated subscript, τ, indicates summation. The choice of F_τ determines the class of 1D CUF model to adopt.
Taylor-like polynomial expansions (TE), $x^i \ z^j$, of the displacement field above the cross-section of the structure represent one of the two 1D CUF classes developed (i and j are positive integers). For example, the second-order model, $N = 2$, has the following kinematic model:

$$\begin{aligned} u_x &= u_{x_1} + x\, u_{x_2} + z\, u_{x_3} + x^2\, u_{x_4} + xz\, u_{x_5} + z^2\, u_{x_6} \\ u_y &= u_{y_1} + x\, u_{y_2} + z\, u_{y_3} + x^2\, u_{y_4} + xz\, u_{y_5} + z^2\, u_{y_6} \\ u_z &= u_{z_1} + x\, u_{z_2} + z\, u_{z_3} + x^2\, u_{z_4} + xz\, u_{z_5} + z^2\, u_{z_6} \end{aligned} \tag{7}$$

The 1D model given by Eq. 7 has 18 generalized displacement variables: three constant, six linear, and nine parabolic terms. The order N of the expansion is arbitrary and is set as an input of the analysis. The choice

of N for a given structural problem is usually made through a convergence study.
LE models exploit Lagrange polynomials to build 1D higher-order theories. In this paper, two types of cross-section polynomial sets were adopted: nine-point elements, L9, and six-point elements, L6. The isoparametric formulation was exploited to deal with arbitrary geometries. The L9 interpolation functions are given by[18]

$$F_\tau = \tfrac{1}{4}(r^2 + r\, r_\tau)(s^2 + s\, s_\tau) \qquad \tau = 1,3,5,7$$

$$F_\tau = \tfrac{1}{2}s_\tau^2(s^2 - s\, s_\tau)(1 - r^2) + \tfrac{1}{2}r_\tau^2(r^2 - r\, r_\tau)(1 - s^2) \qquad \tau = 2,4,6,8 \tag{8}$$

$$F_\tau = (1 - r^2)(1 - s^2) \qquad \tau = 9$$

where r and s range from -1 to $+1$ and where r_τ and s_τ are the natural coordinates of the interpolation points above the cross-section. One component of the displacement field given by an L9 element is

$$u_x = F_1\, u_{x_1} + F_2\, u_{x_2} + F_3\, u_{x_3} + F_4\, u_{x_4} + F_5\, u_{x_5} + F_6\, u_{x_6} + F_7\, u_{x_7} + F_8\, u_{x_8} + F_9\, u_{x_9} \tag{9}$$

where $u_{x_1}, ..., u_{x_9}$ are the displacement variables of the problem and they represent the translational displacement components of each of the nine points of the L9 element. This means that LE models provide elements that only have displacement variables. For the sake of brevity L6 polynomial models are not described here, they can be found in Carrera and Petrolo.[19]

B. FE Formulation and the Fundamental Nucleus

The FE approach was adopted to discretize the structure along the y-axis, this process was conducted via a classical finite element methodology via the Principle of Virtual Displacements. In a compact notation the stiffness matrix can be written as

$$\begin{aligned}
\boldsymbol{K}^{ij\tau s} \;=\; & I_l^{ij} \lhd \left(\boldsymbol{D}_{np}^T F_\tau \boldsymbol{I}\right)\Big[\tilde{\boldsymbol{C}}_{np}\left(\boldsymbol{D}_p F_s \boldsymbol{I}\right) + \tilde{\boldsymbol{C}}_{nn}\left(\boldsymbol{D}_{np} F_s \boldsymbol{I}\right)\Big] + \\
& \left(\boldsymbol{D}_p^T F_\tau \boldsymbol{I}\right)\Big[\tilde{\boldsymbol{C}}_{pp}\left(\boldsymbol{D}_p F_s \boldsymbol{I}\right) + \tilde{\boldsymbol{C}}_{pn}\left(\boldsymbol{D}_{np} F_s \boldsymbol{I}\right)\Big] \rhd_\Omega + \\
& I_l^{ij,_y} \lhd \Big[\left(\boldsymbol{D}_{np}^T F_\tau \boldsymbol{I}\right)\tilde{\boldsymbol{C}}_{nn} + \left(\boldsymbol{D}_p^T F_\tau \boldsymbol{I}\right)\tilde{\boldsymbol{C}}_{pn}\Big] F_s \rhd_\Omega \boldsymbol{I}_{\Omega y} + \\
& I_l^{i,_y j}\, \boldsymbol{I}_{\Omega y} \lhd F_\tau \Big[\tilde{\boldsymbol{C}}_{np}\left(\boldsymbol{D}_p F_s \boldsymbol{I}\right) + \tilde{\boldsymbol{C}}_{nn}\left(\boldsymbol{D}_{np} F_s \boldsymbol{I}\right)\Big] \rhd_\Omega + \\
& I_l^{i,_y j,_y}\, \boldsymbol{I}_{\Omega y} \lhd F_\tau\, \tilde{\boldsymbol{C}}_{nn} F_s \rhd_\Omega \boldsymbol{I}_{\Omega y}
\end{aligned} \tag{10}$$

where

$$\boldsymbol{I}_{\Omega y} = \begin{bmatrix} 0 & 1 & 0 \\ 1 & 0 & 0 \\ 0 & 0 & 1 \end{bmatrix} \qquad \lhd \ldots \rhd_\Omega = \int_\Omega \ldots\, d\Omega \tag{11}$$

$$\left(I_l^{ij}, I_l^{ij,_y}, I_l^{i,_y j}, I_l^{i,_y j,_y}\right) = \int_l \left(N_i N_j,\, N_i N_{j,_y},\, N_{i,_y} N_j,\, N_{i,_y} N_{j,_y}\right) dy \tag{12}$$

$\mathbf{K}^{ij\tau s}$ is the stiffness matrix in the form of the fundamental nucleus, its components can be found in Carrera and Petrolo.[13] It has to be underlined that the formal expression of the fundamental nucleus

- does not depend on the expansion order,
- does not depend on the choice of the F_τ expansion polynomials.

These are the key-points of CUF which permit, with only nine FORTRAN statements, to implement any-order multiple class theories.

C. Component-Wise Approach in the 1D CUF Framework

The present modeling approach is described as *Component-Wise* because each typical component of a composite structure can be modeled through the 1D CUF formulation. In a finite element framework, for instance, this means that layers, fibers and matrices can be modeled by means of the same 1D finite element and therefore, with no need for ad hoc formulations for each component. In other words, the same stiffness matrix ($\mathbf{K}^{ij\tau s}$) is used for each component. Figure 1 provides a description of a possible modeling approach. A four-layer plate is considered and, in top-to-bottom order, the components considered are the following: the first two layers, fibers and matrix of the third layer, the third fiber-matrix cell of the bottom layer and its remaining layer portions. Each component is considered with its own geometrical and material characteristics. In general it can be stated that the CW approach can model a single layer in the following ways:

- As a layer (as the first two layers in Fig. 1).
- As a fiber-matrix system (as the third layer in Fig. 1).
- As a combination of layers and fiber-matrix cells (as the fourth layer in Fig. 1)

These three options can be easily extended to multiple layers as shown in Fig. 1. Each domain (e.g. matrix, fibers, layers) is modeled by means of CUF 1D models, this means that the stiffness matrices of matrix, fibers, layers, etc. are formally identical and, thus, they can be directly assembled. Also, the material characteristics of each component can be separately assigned with no need for homogenization. A typical application of the Component-Wise method (CW) is based on the following analysis approach:

- For a given composite structure, structural analysis is first conducted via classical methods (i.e. equivalent single layer or layer-wise).
- The most critical zones of the structures are detected (e.g. those zones where stress values are critical).
- The component-wise approach is then exploited for those critical portions in order to obtain more precise stress fields with acceptable increments of computational costs.

Independently of the choice of the components to model, both TE and LE can be used. Figure 3 shows the matrices assembly adopted in this paper. In the case of TE, the number of unknown variables is given by the order of the 1D model adopted; if LE is adopted, the number of variables will also depend on the number of L-elements assembled.
Nonhomogeneous structures can be dealt with by two modeling approaches, as in the following:

- An Equivalent Single Component approach (ESC) where the homogenization of the properties of each component is conducted by summing the contributions of each component in the stiffness matrix. It is important to highlight that, if layered structures are considered, the present ESC will provide the Equivalent Single Layer approach (ESL).
- A Component-Wise approach (CW) where the homogenization is just conducted at the interface level. If layered structures are considered, CW will provide the Layer-Wise approach (LW).

Both assembly procedures of the stiffness matrix in the framework of CUF are graphically shown in Fig. 3 in case of layered structures. TE and LE models can be used in an ESC manner. LE models obtain an CW description straightforwardly by considering different sets of L-elements per each component. The homogenization is then conducted at the shared interface cross-section nodes. CW is here obtained only by means of LE.

III. Numerical Results

Various numerical examples are presented and discussed in this section. Preliminary assessments were carried out on simple structures in order to validate the present formulation. Then, a fiber-matrix cell was analyzed with particular attention given to the evaluation of the failure index distributions. Comparisons with results from plate and solid models are provided.

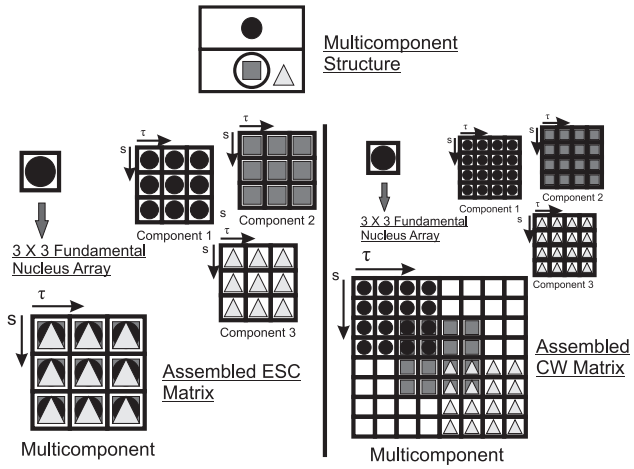

Figure 3. ESC and CW assembly schemes

A. Preliminary assessments

A thin plate was first considered in order to provide preliminary results in terms of failure indexes. The plate cross-section is shown in Fig. 4. The length of the the plate, L, equal to 0.1 m, L/b equal to 10 and L/h equal to 100. The plate was clamped at one end and a vertical point load was applied to the center point of the free tip cross-section, F_z equal to -5.0 N. An orthotropic material was used and its properties are given in Table 1.
Results were evaluated in terms of failure indexes as shown in Tables 2 and 3. Two beam models based on LE expansions were exploited and a plate model from MSC Nastran was used for comparison purposes. An excellent agreement was found between beam and plate results.

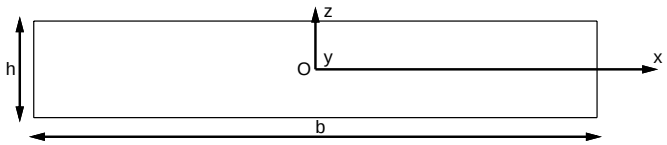

Figure 4. Plate cross-section

Elastic Properties		Stress Limits		Strain Limits	
E_1	127.6 GPa	σ_{11T}	1.730 GPa	ϵ_{11T}	0.0138
E_2, E_3	11.3 GPa	σ_{11C}	1.045 GPa	ϵ_{11C}	0.01175
G_{12}, G_{13}	6.0 GPa	σ_{22T}, σ_{33T}	66.5 MPa	ϵ_{22T}, ϵ_{33T}	0.00436
G_{23}	1.8 GPa	σ_{22C}, σ_{33C}	255.0 MPa	ϵ_{22C}, ϵ_{33C}	0.002
ν_{12}, ν_{13}	0.3	σ_{12}, σ_{13}, σ_{23}	95.1 MPa	ϵ_{12}, ϵ_{13}, ϵ_{23}	0.002
ν_{23}	0.36				

Table 1. Orthotropic material properties

A compact isotropic beam was considered as further preliminary assessment in order to compare the results from 1D CUF with those from a solid finite element model. A square cross-section was considered with $h = 0.1$ mm and $L/h = 10$. The properties of the isotropic material adopted are given in Table 4. The beam was clamped and a vertical force was applied at the center point of the free-tip cross-section, $F_z = -0.1$ N. Three different L9 distributions were implemented as shown in Fig. 5. Fig. 6 shows stress distributions along z and Table 5 presents failure indexes at point A [0, $L/2$, $h/2$] and point C [$b/2$, $L/2$, 0]. It can be stated that there is an excellent agreement between 1D CUF and the solid model and, in particular, the refinement of the L9 distribution improves the shear stress and the failure index detection significantly.

	1 L9	3×3 L9	Plate
	$z = +h/4$		
Max Stress	0.077	0.077	0.077
Max Strain	0.191	0.121	0.121
Tsai-Wu	-0.033	-0.031	-0.032
	$z = -h/4$		
Max Stress	0.128	0.128	0.128
Max Strain	0.089	0.091	0.089
Tsai-Wu	0.052	0.049	0.052

Table 2. Failure indexes at $x = b/2$, $y = L/10$, thin plate

	1 L9	3×3 L9	Plate
	$z = +h/4$		
Max Stress	0.080	0.079	0.077
Max Strain	0.200	0.191	0.146
Tsai-Wu	-0.033	-0.040	-0.038
	$z = -h/4$		
Max Stress	0.132	0.131	0.130
Max Strain	0.092	0.091	0.091
Tsai-Wu	0.053	0.060	0.060

Table 3. Failure indexes at $x = 0$, $y = L/10$, thin plate

Elastic Properties		Stress Limits		Strain Limits	
E	127.6 GPa	σ_T	1.730 GPa	ϵ_T	0.0138
ν	0.3	σ_C	1.045 GPa	ϵ_C	0.01175
		σ_{12}	95.1 MPa	ϵ_{12}	0.002

Table 4. Isotropic material properties

B. Fiber-Matrix Cell

A fiber-matrix cell is considered in this section. This model was retrieved from a previous work by Carrera et al.[16] where a detailed analysis of the displacement and stress fields was carried out. In this work attention was given to the failure index distributions. Fig. 7 shows the cross-section geometry of the square cell where $d = 0.08$ mm, $b = 0.1$ mm and $L/b = 10$. Two isotropic materials were employed as shown in Table 6. The beam was clamped at one end and a vertical force was applied at the center point of the free-tip, $F_z = -0.1$ N. Analyses were carried out by means of Taylor (TE) and Lagrange (LE) 1D CUF models, a solid finite element model was used for comparison purposes. Fig. 8 shows the L-elements distribution employed for the LE model. Table 7 presents the total number of degrees of freedom employed by the models exploited for this analysis.

Table 8 shows displacement and stress values evaluated at different points: point A ($b/2$, L, 0), point B ($b/2$, $L/2$, $d/2$) and point D ($d/2$, $L/2$, 0). Stress and strain distributions above the clamped cross-section are shown in Figs. 9, 10, 11 and 12. Failure index values are given in Table 9 at point B ($b/2$, 0, $d/2$) and point D ($d/2$, 0, 0) whereas the distributions above the clamped cross-section are shown in Figs. 13, 14 and 15. The results obtained suggest the following:

- A general good agreement was found between the 1D CUF and the solid finite element model.

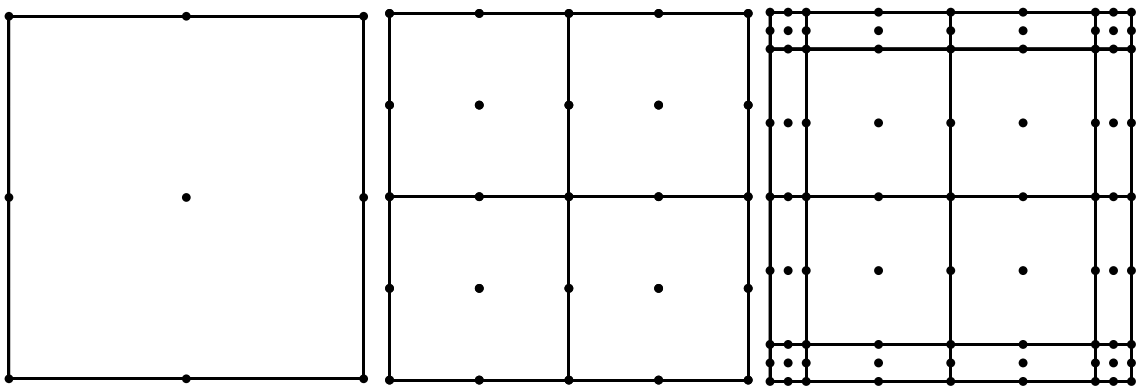

Figure 5. Isotropic beam L9 distributions: 1 L9, 4 L9 and 16 L9

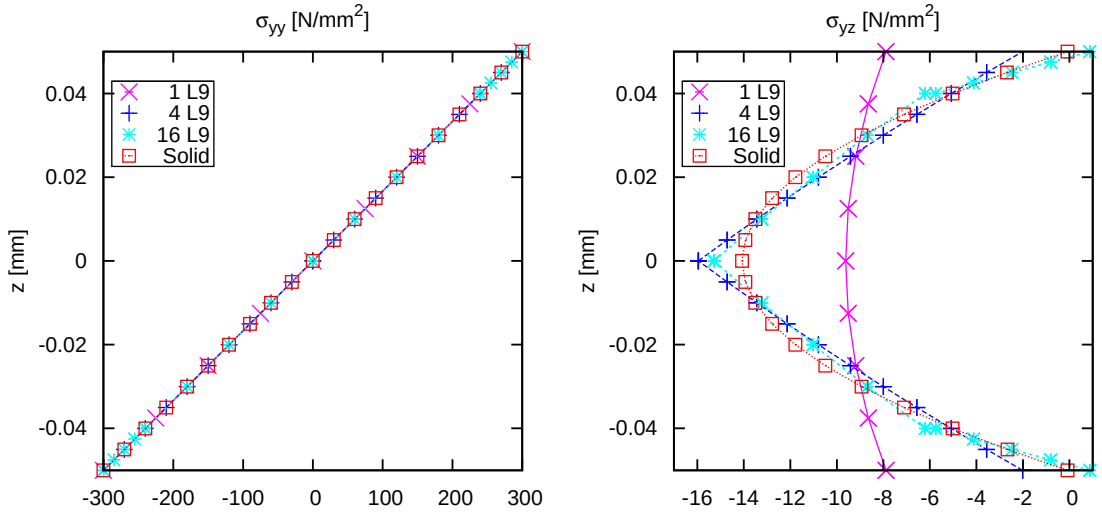

Figure 6. Axial (σ_{yy}) and shear (σ_{yz}) stress at $y = L/2$, $x = 0$ for the isotropic beam

- 1D CUF LE is able to detect 3D-like stress, strain and failure index fields.
- The computational costs of CUF models are extremely lower than those of solid models.

	Point A			
	1 L9	4 L9	16 L9	SOLID
Max Stress	0.1734	0.1734	0.1731	0.17341
Max Strain	0.1704	0.1704	0.1701	0.17037
	Point C			
	1 L9	4 L9	16 L9	SOLID
Max Stress	0.1314	0.2077	0.1955	0.18184
Max Strain	0.1274	0.2013	0.1894	0.17619

Table 5. Failure indexes for the isotropic beam at $L/2$

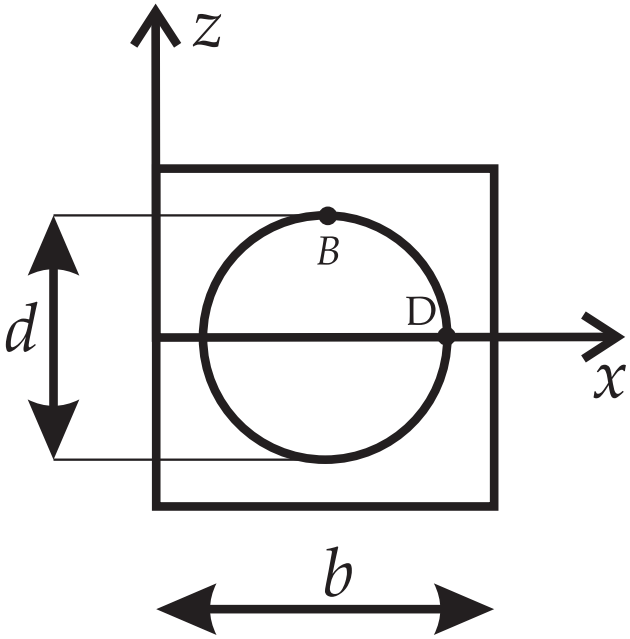

Figure 7. Fiber-Matrix cell geometry.

Elastic Properties		Stress Limits		Strain Limits	
		Fiber			
E	250.6 GPa	σ_T	3.398 GPa	ϵ_T	0.0138
ν	0.2456	σ_C	2.053 GPa	ϵ_C	0.01175
		σ_{12}	186.8 MPa	ϵ_{12}	0.004
		Matrix			
E	3.252 GPa	σ_T	66.5 MPa	ϵ_T	0.00436
ν	0.355	σ_C	255.0 GPa	ϵ_C	0.002
		σ_{12}	74.0 MPa	ϵ_{12}	0.0016

Table 6. Fiber-Matrix material properties

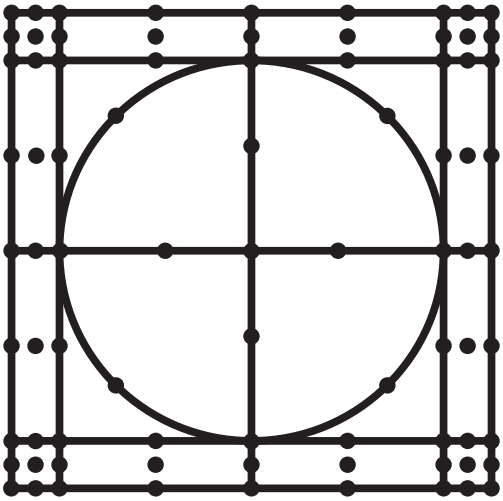

Figure 8. L-Elements distribution for the fiber-matrix cell: 12 L9 + 8 L6

Model	DOFs
Classical Beam Models	
EBBT	363
TBT	605
TE	
$N = 1$	1089
$N = 2$	2178
$N = 3$	3630
$N = 4$	5445
$N = 5$	7623
$N = 6$	10164
$N = 7$	13068
$N = 8$	16335
LE	
12 L9 + 8 L6	7533
SOLID	
	268215

Table 7. Number of degrees of freedom of each finite element model for the fiber-matrix cell

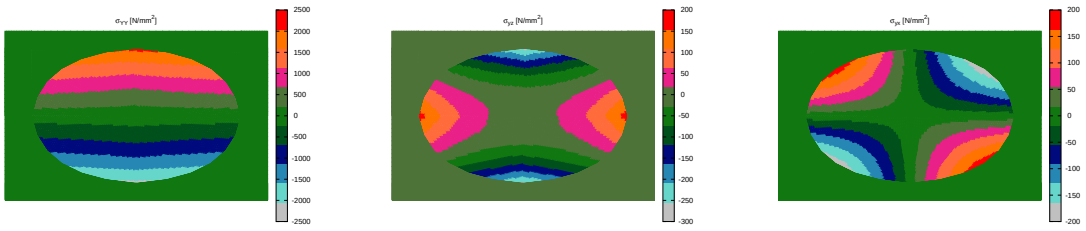

(a) σ_{yy} (b) σ_{yz} (c) σ_{yx}

Figure 9. Axial and shear stresses at $y = 0$ for the fiber-matrix cell, LE model

Model	$u_z \times 10^2$ mm Point A	$\sigma_{yy} \times 10^{-2}$ MPa Point B	$\sigma_{yz} \times 10^{-2}$ MPa Point D
		Classical Beam Model	
EBBT	−6.356	9.558	−1.966
TBT	−6.376	9.558	−1.966
		TE	
N = 1	−6.376	9.558	−1.966
N = 2	−6.335	9.487	−2.353
N = 3	−6.338	9.487	−2.481
N = 4	−6.345	9.447	−2.475
N = 5	−6.345	9.447	−2.407
N = 6	−6.349	9.431	−2.406
N = 7	−6.349	9.431	−2.348
N = 8	−6.350	9.455	−2.348
		LE	
12 L9 + 8 L6	−6.440	9.451	−2.551
		SOLID	
	−6.357	9.531	−2.428

Table 8. Displacement and stress values for the fiber-matrix cell

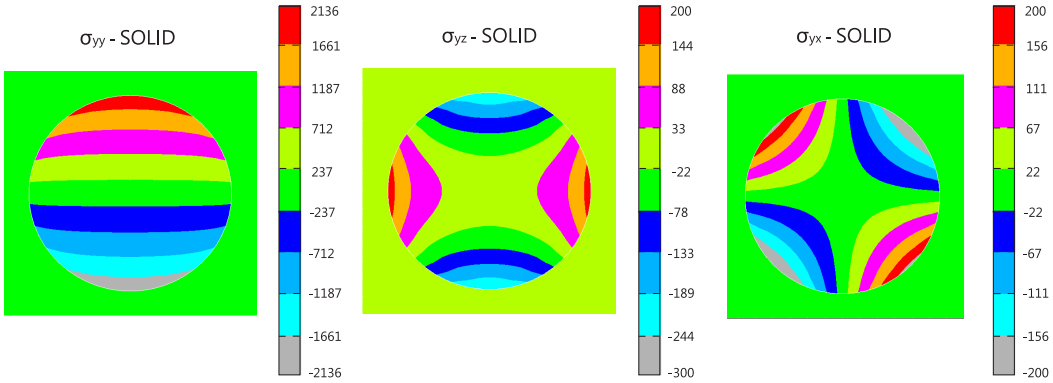

(a) σ_{yy} (b) σ_{yz} (c) σ_{yx}

Figure 10. Axial and shear stresses at $y = 0$ for the fiber-matrix cell, solid model

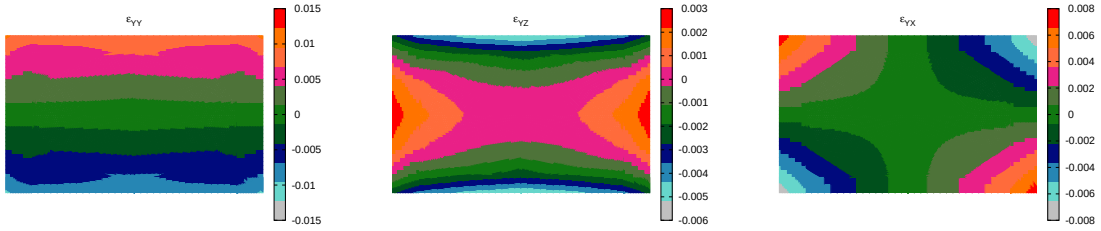

(a) ϵ_{yy} (b) ϵ_{yz} (c) ϵ_{yx}

Figure 11. Axial and shear strains at $y = 0$ for the fiber-matrix cell, LE model

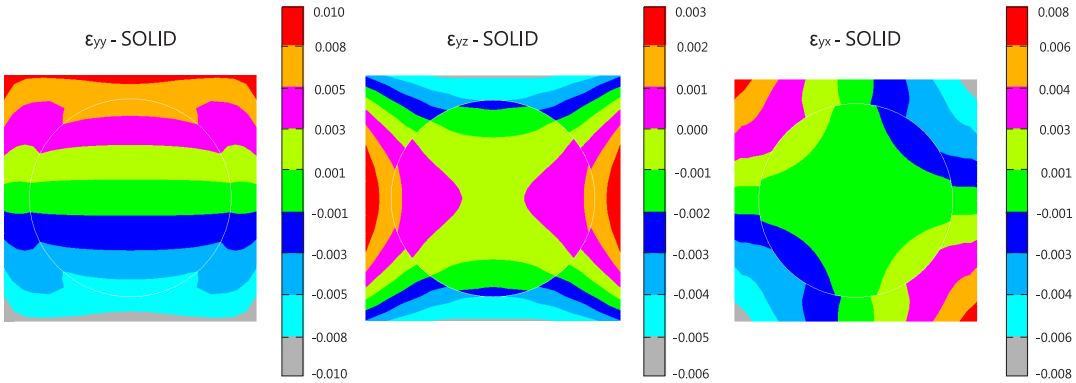

(a) ϵ_{yy} (b) ϵ_{yz} (c) ϵ_{yx}

Figure 12. Axial and shear strains at $y = 0$ for the fiber-matrix cell, solid model

	Point B	
	12 L9+8 L6	SOLID
Max Stress	1.44	1.30
Max Strain	0.67	0.60
Tsai-Wu	1.68	1.42
Tsai-Hill	1.50	1.50
	Point D	
	12 L9+8 L6	SOLID
Max Stress	0.95	0.96
Max Strain	0.44	0.44
Tsai-Wu	0.89	0.93
Tsai-Hill	0.95	0.93

Table 9. Failure indexes for the fiber-matrix cell

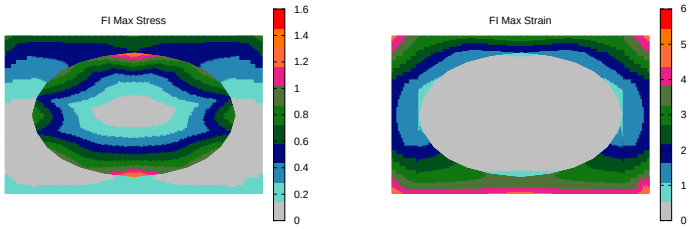

(a) Maximum stress (b) Maximum strain

Figure 13. Failure indexes for the fiber-matrix cell, LE model

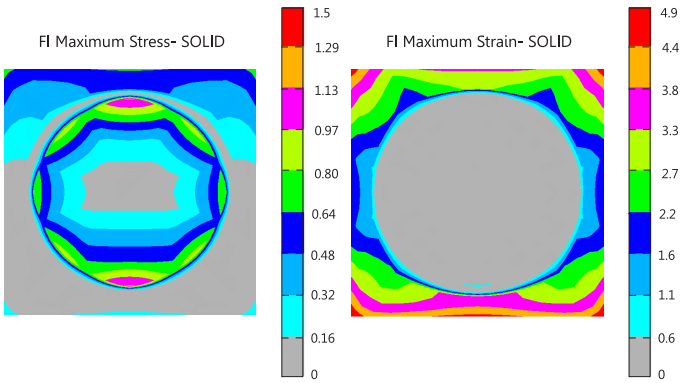

(a) Maximum stress (b) Maximum strain

Figure 14. Failure indexes for the fiber-matrix cell, solid model

IV. Conclusion

Failure indexes of fiber reinforced composite structures are computed in this work. Analyses were conducted by means of the Component-Wise approach (CW) and 1D refined structural models. 1D CW was developed within the framework of the Carrera Unified Formulation (CUF) which is a modeling tool able to deal with any-order structural models in a unified manner. The 1D structural models exploited in this work can model laminates, laminae, fibers and matrices separately, that is, different scale components can

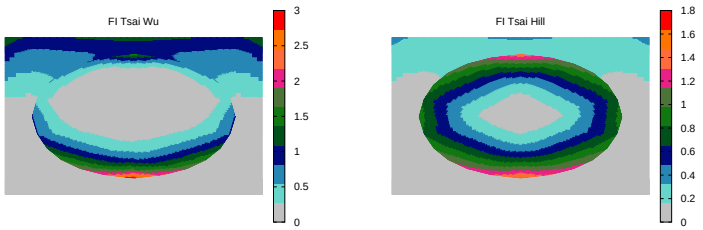

(a) Tsai-Wu (b) Tsai-Hill

Figure 15. Tsai-Wu and Tsai-Hill failure index distributions, LE model

be modeled by using the same 1D formulation. Particular attention was given to a simple fiber-matrix cell unit in order to highlight the analysis capabilities of the formulation proposed. Comparisons with results from 3D solid models were provided. The results obtained suggest the following.

- The proposed CW approach can detect 3D-like stress fields of fiber-matrix cells.
- The present 1D formulation is extremely advantageous in terms of computational costs if compared to solid models.
- The advantages in terms of computational costs can be even larger if a global-local approach is considered where detailed fiber-matrix cells are employed in portions of the entire structure.

As a general guideline, the CW approach should be adopted in a global-to-local analysis scenario where results from globally refined models are exploited to evaluate the most critical areas of a given structure and where locally refined models are then employed to obtain accurate stress fields in those critical areas. CW should also be employed for damage analyses in future investigations.

References

[1]Orifici, A., Herszberg, I., and Thomson, R., "Review of methodologies for composite material modelling incorporating failure," *Composite Structures*, Vol. 86, 2008, pp. 194–210, DOI:10.1016/j.compstruct.2008.03.007.

[2]Kapania, K. and Raciti, S., "Recent Advances in Analysis of Laminated Beams and Plates, Part I: Shear Effects and Buckling," *AIAA Journal*, Vol. 27, No. 7, 1989, pp. 923–935.

[3]Lekhnitskii, S., "Strength calculation of composite beams," *Vestnik inzhen i tekhnikov*, Vol. 9, 1935.

[4]Carrera, E., "Historical review of Zig-Zag theories for multilayered plates and shells," *Applied Mechanics Review*, Vol. 56, No. 3, 2003, pp. 287–308.

[5]Robbins Jr., D. and Reddy, J., "Modeling of thick composites using a layer-wise theory," *International Journal of Numerical Methods in Engineering*, Vol. 36, 1993, pp. 655–677.

[6]Carrera, E., "Evaluation of layer-wise mixed theories for laminated plates analysis," *AIAA Journal*, Vol. 36, 1998, pp. 830–839.

[7]Mourad, H., Williams, T., and Addessio, F., "Finite element analysis of inelastic laminated plates using a globallocal formulation with delamination," *Comput. Methods Appl. Mech. Engrg.*, Vol. 198, 2008, pp. 542–554.

[8]Ben Dhia, H. and Rateau, G., "The Arlequin method as a flexible engineering design tool," *International Journal of Numerical Methods in Engineering*, Vol. 62, No. 11, 2005, pp. 1442–1462.

[9]Biscani, F., Giunta, G., Belouettar, S., Carrera, E., and Hu, H., "Variable kinematic beam elements coupled via Arlequin method," *Composite Structures*, Vol. 93, No. 2, 2011, pp. 697–708.

[10]Lu, G. and Kaxiras, E., *Handbook of Theoretical and Computational Nanotechnology*, Vol. X, American Scientific Publishers, 2005.

[11]Aboudi, J., *Mechanics of Composite Materials: A Unified Micromechanical Approach*, Elsevier, 1991.

[12]Pineda, E., Waas, A., Bednarcyk, B., Collier, C., and P.W., Y., "Progressive damage and failure modeling in notched-laminated fiber reinforced composites," *International Journal of Fracture*, Vol. 158, No. 2, 2009, pp. 125–143.

[13]Carrera, E. and Petrolo, M., "On the Effectiveness of Higher-Order Terms in Refined Beam Theories," *Journal of Applied Mechanics*, Vol. 78, No. 3, 2011, doi: 10.1115/1.4002207.

[14]Carrera, E. and Petrolo, M., "Refined One-Dimensional Formulations for Laminated Structure Analysis," *AIAA Journal*, Vol. 50, No. 1, 2012, DOI: 10.1007/s11012-011-9466-5.

[15]Carrera, E., Giunta, G., and Petrolo, M., *Beam Structures: Classical and Advanced Theories*, John Wiley & Sons, 2011.

[16]Carrera, E., Maiaru', M., and Petrolo, M., "One-Dimensional Hierarchical Formulation for Component-Wise Analysis of Laminated Anisotropic Composites," *International Journal of Solids and Structures*, 2012, doi: 10.1016/j.ijsolstr.2012.03.025.

[17]Carrera, E., Petrolo, M., and Zappino, E., "Performance of CUF approach to analyze the structural behavior of slender bodies," *Journal of Structural Engineering*, Vol. 138, No. 285, 2012, doi:10.1061/(ASCE)ST.1943-541X.0000402.

[18]Oñate, E., *Structural Analysis with the Finite Element Method: Linear Statics, Volume 1*, Springer, 2009.

[19]Carrera, E. and Petrolo, M., "Refined Beam Elements with only Displacement Variables and Plate/Shell Capabilities," *Meccanica*, Vol. 47, No. 3, 2012, DOI: 10.1007/s11012-011-9466-5.